

DICE: Staleness-Centric Optimizations for Efficient Diffusion MoE Inference

Jiajun Luo¹, Lizhuo Luo², Jianru Xu², Jiajun Song¹, Rongwei Lu¹, Chen Tang³, Zhi Wang¹
¹Tsinghua University ²SUSTech ³The Chinese University of Hong Kong

luo-jj24@mails.tsinghua.edu.cn

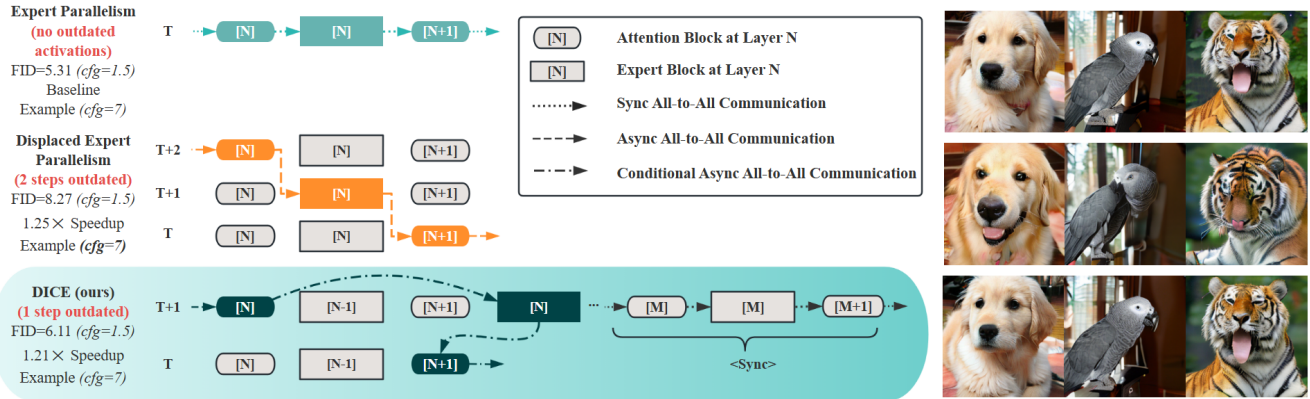


Figure 1. We introduce **DICE**, a framework designed to enhance scalability and efficiency in MoE-based diffusion models. **DICE** perform staleness-centric optimizations through *Interweaved Parallelism*, *Selective Synchronization*, and *Conditional Communication*. It achieves up to 1.2 \times speedup with minimal quality loss. Left: Architectural comparison. Right: Visual quality results.

Abstract

Mixture-of-Experts-based (MoE-based) diffusion models have shown their scalability and ability to generate high-quality images, making them a promising choice for efficient model scaling. However, they rely on expert parallelism across GPUs, necessitating efficient parallelism optimization. While state-of-the-art diffusion parallel inference methods overlap communication and computation via displaced operations, they introduce substantial **staleness**—the utilization of outdated activations, which is especially severe in expert parallelism scenarios and leads to significant performance degradation. We identify this staleness issue and propose **DICE**, a staleness-centric optimization with a three-fold approach: (1) *Interweaved Parallelism* reduces step-level staleness for free while overlapping communication and computation; (2) *Selective Synchronization* operates at layer-level and protects critical layers vulnerable from staled activations; and (3) *Conditional Communication*, a token-level, training-free method that dynamically adjusts communication frequency based on token importance. Together, these optimizations effectively reduce staleness, achieving up to 1.2 \times speedup with minimal quality degradation. Our results establish **DICE** as an effective, scalable solution for large-scale MoE-based diffusion model inference.

1. Introduction

Diffusion models [3, 13, 31, 37] have revolutionized the field of generative modeling, enabling the creation of high-fidelity images [15, 38] and videos [14, 24, 35] that rival human creativity in quality and detail. Among the architectures, the Diffusion Transformer (DiT) [29, 39] with Mixture-of-Experts (MoE) [34] stands out due to its effectiveness in scalability. MoE enables large diffusion models to expand capacity with sub-linear cost increases by dividing the model into multiple experts, only a subset of which are activated for each input. This selective activation reduces computational overhead, allowing MoE models to achieve high performance at a lower cost by engaging only the necessary experts per input. As demonstrated by DiT-MoE [6], MoE-based diffusion models have been scaled to 16 billion parameters with improved generation quality.

Scaling MoE-based diffusion models necessitates expert parallelism [17, 30] to handle their extensive memory footprint; however, it also introduces significant communication bottlenecks. By distributing experts across multiple GPUs, expert parallelism substantially reduces the memory usage for very large models [4]. While this approach optimizes memory utilization, it incurs substantial communication overhead due to synchronized token exchanges [10, 18, 19, 42] (as shown in Figure 2, two all-to-all communications are required each layer). This communi-

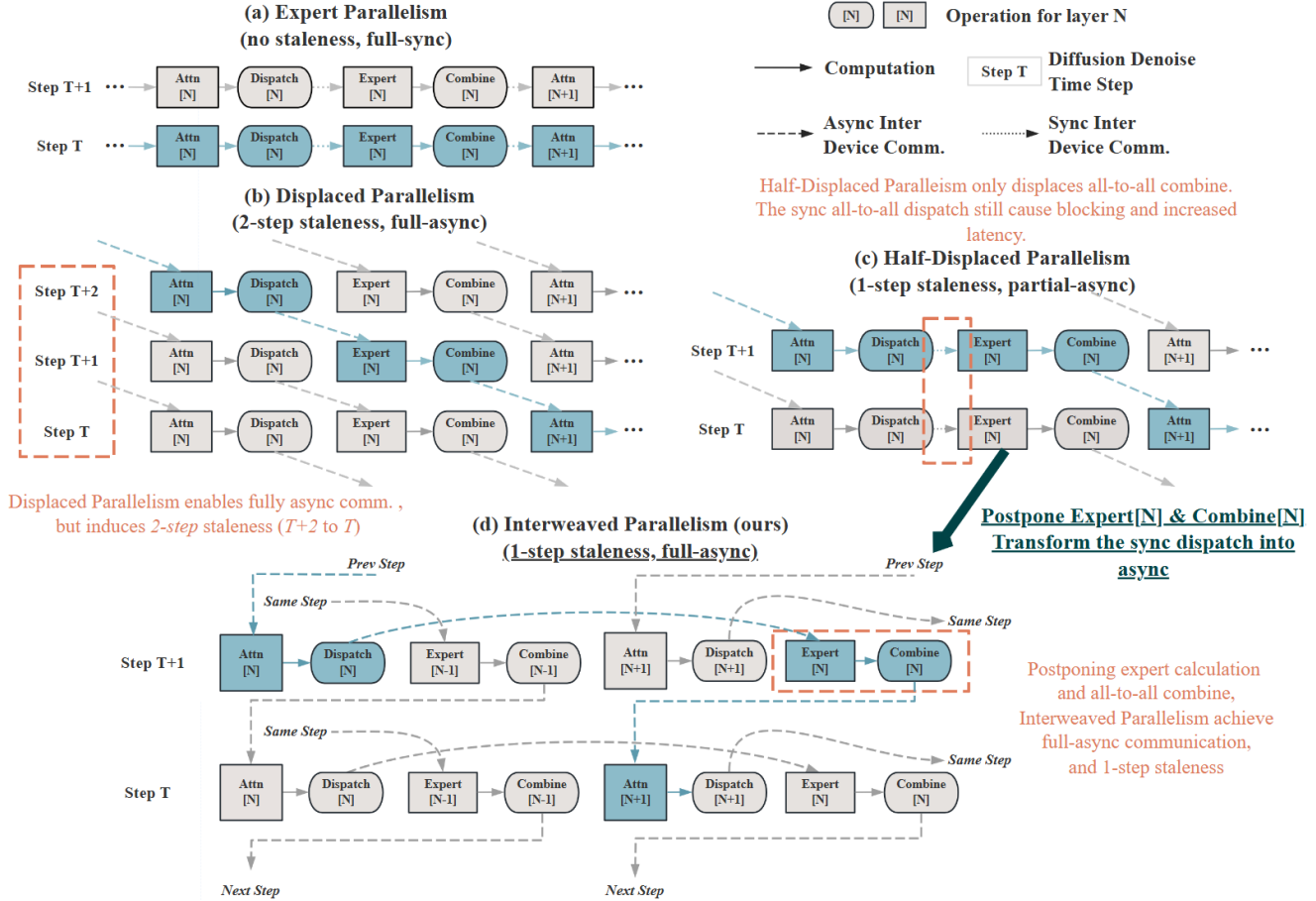


Figure 2. Comparison of parallelism methods for MoE-based diffusion models. Here, we use Half-Displaced Parallelism to illustrate the transition to Interweaved Parallelism, demonstrating how adjustments in communication and computation timing lead to reduced staleness while maintaining asynchronous efficiency. The highlighted sections show the origin of activations used in Step T .

communication presents a major challenge for MoE-based diffusion inference.

To address communication challenges in parallel inference, state-of-the-art methods employ *Displaced Parallelism* [21]. This approach leverages the similarity between activations of the same layer across successive steps to reduce communication blocking time. This similarity allows displaced parallelism to avoid the wait time associated with synchronous communication. Instead of halting computations until the latest activations are received, it sends activations in an asynchronous, non-blocking manner. Meanwhile, it immediately proceeds with computations using slightly outdated (*stale*) activations from the previous step, which are similar enough to serve as a close approximation of the current data. This approach enables continuous computation across devices, effectively reducing idle time by overlapping communication and computation. As depicted in Figure 2, the dispatch operation at step $T + 1$ can bypass waiting for the latest data by directly using the ac-

tivations sent in advance from step $T + 2$ (the highlighted dispatch). This advanced transmission enables continuous computation across devices, effectively reducing idle time by overlapping communication and computation.

However, displaced parallelism introduces the issue of **staleness**—the utilization of activations from earlier steps instead of real-time data—which can significantly degrade model performance, increasing the Fréchet Inception Distance (FID) score from 5.31 to 8.27 (detailed in Section 5). Staleness occurs because asynchronous communication delays the usage of activations until a future step, causing layers to compute based on outdated information.

We quantify staleness as the *difference in steps between when the input was generated and the step in which its corresponding output is used*. Displaced parallelism exhibits 2-step staleness, as the result used in Step T is driven by activations from Step $T + 2$ in the same layer (highlighted in Figure 2), relying on outdated data. Our method reduces this to 1 step, ensuring fresher activations.

We conduct an in-depth analysis of the staleness phenomenon in MoE parallelism and derive several key insights. At the step level, we find an optimized parallel scheme to halve the staleness compared to displaced parallelism without incurring any overhead. At the layer level, we observe that, due to the characteristics of vision tasks, different MoE layers exhibit varying sensitivity to staleness introduced by asynchronous communication; deeper layers are more sensitive, while shallow layers are more tolerant. At the token level, we discover that introducing staleness to important tokens significantly degrades the overall image quality, whereas less critical tokens cause less degradation.

Based on these findings, we propose **DICE** (Diffusion Inference with staleness-**C**entric optimizations), which enhances parallel inference at the step, layer, and token granularities. **DICE** incorporates a three-fold approach to manage staleness effectively: (1) *Interweaved Parallelism* reduces step-level staleness by half (from two steps to one) compared to displaced parallelism, halving the required buffer size, and achieving this without any overhead. Detailed in Figure 2. (2) *Selective Synchronization* synchronizes only the layers most sensitive to staleness, ensuring that critical information remains up-to-date; and (3) *Conditional Communication*, a token-aware strategy that adjusts communication frequency based on token importance. It leverages existing MoE routers and thus is training-free. Together, these optimizations mitigate staleness issues while enhancing memory usage and inference efficiency, achieving up to a $1.2\times$ speedup with minimal quality impact.

To summarize, our contributions are as follows:

- We are the first to identify the issue of staleness in MoE-based diffusion model inference, highlighting its impact on performance.
- We conduct a comprehensive analysis of staleness, revealing these key insights: optimizing the parallel scheme can reduce staleness for free at the step level; deeper MoE layers are more sensitive to staleness at the layer level, and certain tokens are more adversely affected by staleness at the token level.
- Based on these insights, we propose **DICE**, which optimizes staleness at the step, layer, and token granularities through interweaved parallelism, selective synchronization, and conditional communication, respectively. **DICE** outperforms state-of-the-art methods, providing a cohesive framework to improve the quality, efficiency, and scalability of parallel inference. The code will be publicly available.
- We validate our solution across diverse configurations, including multiple model sizes and baselines, demonstrating substantial speedups and high image quality.

2. Preliminaries & Related Works

2.1. MoE-based Diffusion Models

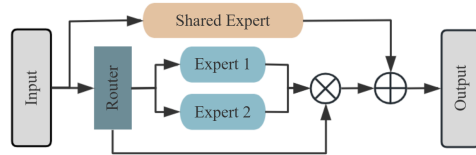


Figure 3. Illustration of an MoE model[6]

Mixture-of-Experts (MoE) [34] is an architecture that efficiently scales model capacity by partitioning the network into multiple specialized experts, with only a subset activated for each input, as depicted in Figure 3. DiT-MoE[6] integrates MoE into Diffusion Transformers to effectively scale diffusion models to 16.5 billion parameters. It also employs shared experts to capture common knowledge[30]. The largest DiT-MoE model features 32 experts and achieves state-of-the-art performance on ImageNet [2].

2.2. Displaced Parallelism

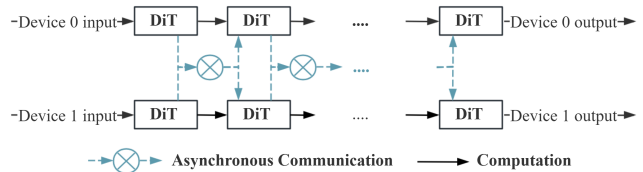


Figure 4. Illustration of displaced parallelism in DiT across multiple devices, with dashed arrows representing asynchronous communication steps that defer data exchange until the next computation stage.

Displaced Parallelism, introduced by DistriFusion [21], leverages activation similarity between successive diffusion steps to asynchronously transfer activations, effectively overlapping communication and computation for significant speedup. As shown in Figure 4, activations computed in the current step are sent asynchronously and used in the next step. However, this approach introduces staleness due to deferred communication, leading to quality degradation, especially in expert parallelism. To address this, we introduce staleness-centric optimizations that enhance efficiency and maintain output quality.

Subsequent works like PipeFusion [40] and AsyncDiff [1] also exploit activation similarity to accelerate diffusion inference. In addition to displaced parallelism, caching methods have been proposed as alternative optimizations targeting U-Net [8, 26, 36, 41], DiT [33], and learned caching [25].

2.3. Expert Parallelism

Expert Parallelism [17] is a strategy specifically designed for MoE models, distributing experts across different devices, with each handling a subset of experts. For non-MoE layers, it functions like data parallelism, where each device processes its batch independently. In MoE layers, tokens are dynamically routed to the devices of their assigned experts, requiring two inter-device all-to-all for token exchanges. Expert parallelism enables efficient memory utilization for scaling huge models.

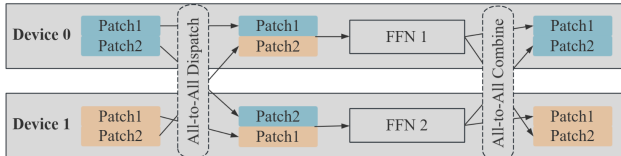


Figure 5. Visualization of expert parallelism.

Given the dominant performance of MoE in a wide range of tasks and the necessity of expert parallelism in its inference and pre-training, optimizing expert parallelism has been a critical topic. FasterMoE [10] mitigates communication bottlenecks by implementing pipelined all-to-all communication and tackling expert imbalance through expert shadowing. DeepSpeed-MoE [30] leverages efficient parallel communication and model compression techniques. BASE Layers [18] use distributed linear assignment to enforce balanced token-to-expert allocation. Additionally, various works utilize topology-aware token routing to handle communication bottleneck [10, 20].

However, none of these methods have been specifically tailored for diffusion models, nor do they address the unique staleness challenges that arise in expert parallelism within diffusion processes. Our work fills this gap by introducing staleness-centric optimizations tailored for MoE-based diffusion models, effectively reducing staleness and improving inference efficiency.

3. Motivation

Our motivation is based on three key observations: first, the communication bottleneck in expert parallelism highlights the necessity for communication optimization; second, we observed high similarity in input/output and routing, suggesting the feasibility of optimization through asynchronous communication; and third, we identified staleness as the core issue in optimization, presenting the main challenge to performance.

Communication bottleneck in expert parallelism. All-to-all operations in expert parallelism introduce significant communication overhead, presenting a major bottleneck [42]. Our evaluation of DiT-MoE-XL on 8 GPUs shows that all-to-all communication accounts for a substan-

tial portion of the total inference time. Specifically, for batch sizes 4, 8, and 16, the all-to-all communication times were 15.91 seconds (61.7% of the total time), 28.99 seconds (69.8%), and 54.94 seconds (73.3%), respectively, highlighting the necessity to mitigate the communication inefficiency.

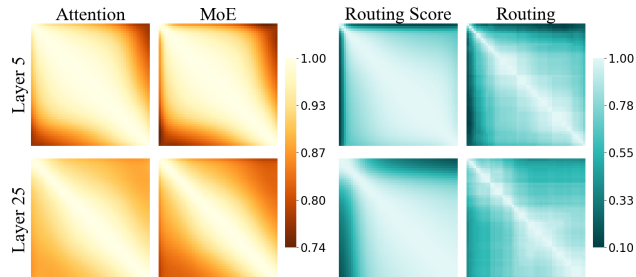


Figure 6. Visualization of similarity between different diffusion steps in DiT-MoE. The images represent the MoE input features, MoE output features, route scores of selected layers and router assignment. We use a one-hot encoding to represent expert assignments, which enables computing similarity as the discrete tensor’s similarity measure.

Similarity in MoE-based diffusion models. The sequential denoising process in diffusion models limits inference speed, but recent approaches leverage feature redundancy to enhance efficiency [25, 26]. We observe that in the DiT-MoE model, there is an inherent similarity in MoE gate activations and token routing decisions between adjacent diffusion steps (see Figure 6). This consistent activation and routing suggest redundant computations, revealing the potential for optimization by reusing routing information in expert parallelism.

Staleness degrades performance. We discovered that using outdated(staled) activations due to communication delays in expert parallelism severely degrades model performance. Displaced parallelism induces a two-step staleness in expert parallelism, which causes a notable drop in image quality: the FID score increases from 5.31 to 8.27. Our staleness-centric optimizations decrease staleness to just one step, along with efficient staleness trade-offs, leading to significant speedup and quality improvement.

4. Methodology

Scaling MoE-based diffusion models effectively require managing the staleness induced by parallelism methods. Existing approaches, such as displaced parallelism, enable communication-computation overlap but at the cost of significant staleness in token activations, which degrades model performance.

We propose **DICE**, a staleness-centric solution designed to reduce staleness on step, layer, and token levels. We introduce a three-fold optimization strategy: *Interweaved*

Parallelism, Selective Synchronization, and Conditional Communication. Each component addresses a distinct level of staleness, providing a cohesive framework to boost efficiency and performance.

4.1. Interweaved Parallelism

Our first optimization, *Interweaved Parallelism*, redefines the timing of communication and computation to reduce step-level staleness.

In Expert Parallelism, tokens are dispatched via an all-to-all operation to designated experts across devices, processed by local experts, and then returned to their original devices through another all-to-all combine operation. This synchronous process incurs considerable latency, impacting inference speed.

State-of-the-art methods use displaced parallelism [21, 40] to overlap communication and computation in distributed diffusion inference. By asynchronously initiating communication in one step and using the results in the subsequent step, it reduces blocking time.

However, displaced parallelism results in a two-step staleness, causing severe quality degradation: tokens dispatched in one step only reach their designated experts in the next, and the results are then combined two steps later.

The proposed **interweaved parallelism reduces staleness by half compared to displaced parallelism**, achieving a one-step staleness instead of two. In our approach, the asynchronous all-to-all dispatch is launched at each step asynchronously but is not deferred to the subsequent step for processing. Instead, the results of the dispatch operation are utilized in the following stage within the same step, as depicted in Figure 7. After processing by the expert, the results are sent to the next step. This method effectively reduces the staleness to a single step, compared to the two-step staleness seen in displaced parallelism. The structure of interweaved parallelism creates a flow where the expert processing and remaining model layers are “interwoven” As each step progresses, computation alternates between current-layer processing and the expert output from the prior layer, which allows for streamlined data flow.

Interweaved parallelism offers a comparable overlap to displaced parallelism without the need for a full-step delay. While displaced parallelism offsets the entire expert processing by one step, the actual expected overlap remains similar, with each all-to-all communication phase effectively overlapping with the computation of one layer. Thus interweaved parallelism reduces staleness without increased latency. Furthermore, it **halves the buffer size**, as only the combine results need to be stored for the next step, unlike displaced parallelism, which requires both dispatch and combine results to be kept until the subsequent step.

Compared to state-of-the-art methods, interweaved parallelism achieves better image quality by halving staleness,

improves memory efficiency with halved buffer size, and incurs **no additional latency**.

4.2. Selectively Synchronize Vulnerable Layers

At the layer level, selectively synchronizing vulnerable layers can significantly improve image quality. Our analysis reveals that staleness affects shallow and deep layers differently in MoE-based diffusion models. Specifically, shallow layers primarily extract low-level features, which are less complex and less impacted by staleness introduced through asynchronous communication. In contrast, deeper layers are responsible for capturing higher-level semantics, requiring precise and fresh expert outputs due to the increased complexity and importance of these representations.

Previous work DeepSpeed-MoE [30], observed that in language models, deeper layers benefit more from MoE architectures. Inspired by these findings, we recognize that in visual tasks, staleness in deeper layers due to asynchronous expert parallelism can severely compromise high-level semantic understanding.

To address this, we propose *Selective Synchronization*, which synchronizes only the more vulnerable deeper layers while allowing shallow layers to continue asynchronously. This targeted approach ensures that deeper layers benefit from up-to-date information without the need for full synchronization. Our experiments validate its effectiveness, as shown in Figure 8. Detailed results are presented in Section 5.3.

4.3. Freshness-Latency Trade-Off via Conditional Communication

Our analysis reveals that token-level staleness can be significantly mitigated to greatly reduce latency by adjusting communication based on token importance. Specifically, we found that not all tokens contribute equally to the output in MoE-based diffusion models; tokens with higher router scores have a greater impact on model performance. This insight allows us to prioritize communication for important tokens, thereby reducing unnecessary data transfer without sacrificing quality.

Building on this, we propose *Conditional Communication*, a token-aware, training-free approach that adjusts communication frequency based on token importance. For each token at every step, we always transmit the activation corresponding to its top-scoring expert to ensure freshness for critical tokens. For lower-scoring experts, instead of always transmitting their activations, we reduce the communication frequency by reusing cached results from previous steps, updating them less frequently (e.g., every few steps), as depicted in Figure 7. This selective communication reduces overhead while maintaining performance by keeping important tokens up-to-date and selectively updating less critical ones.

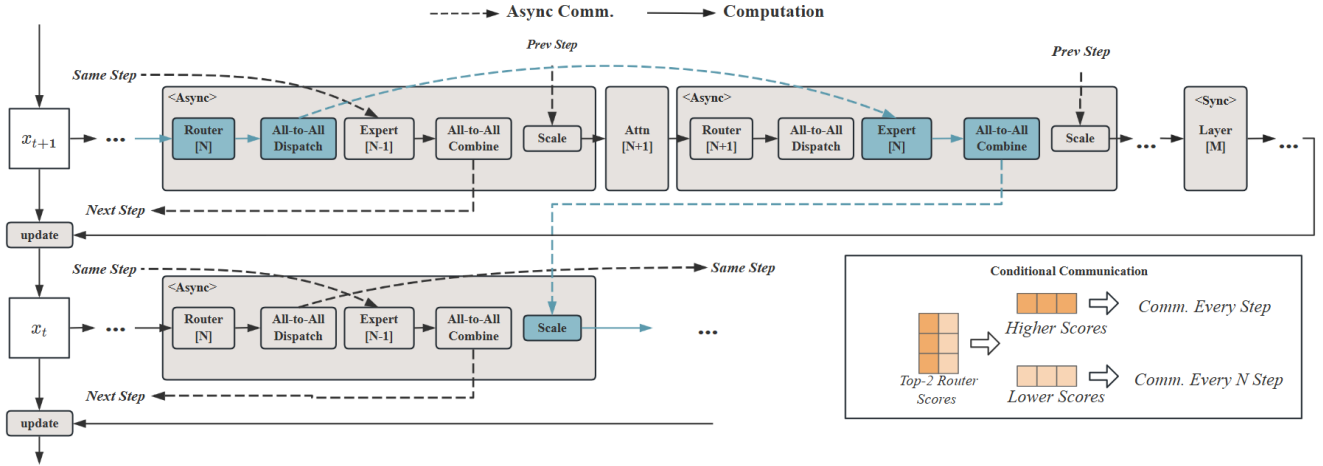


Figure 7. Overview of **DICE**. The highlighted part indicates the path taken by the activations used in step T . *Interweaved Parallelism* postpones the use of the all-to-all dispatch results, while delaying the combine operation by an entire step. It induces a one-step staleness, half of displaced parallelism[21]. *Selective Synchronization* synchronizes staleness-vulnerable deeper layers. *Conditional Communication* assigns higher priority to important tokens based on their router scores, while tokens with lower scores are communicated less frequently.

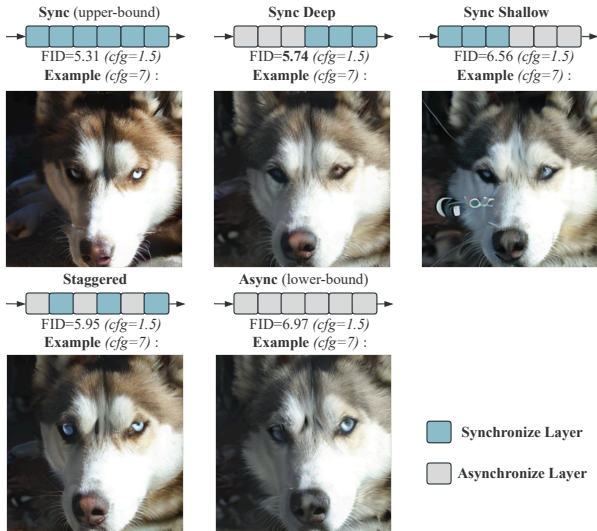


Figure 8. Visual comparison of synchronization strategies in DiT-MoE-XL. Synchronizing only the deep layers provides the most effective optimization. FID shown for $cfg = 1.5$.

Through this strategy, we trade freshness for reduced communication with minimal reduction in overall quality. Experimental comparisons between various strategies confirm that prioritizing high-score tokens yields the best quality and efficiency balance. Further results are detailed in Section 5.3.

4.4. Periodical Synchronization.

We apply a lightweight strategy, synchronizing all layers’ activations periodically across every few steps. This strategy reduces the cumulative staleness impact while preserving the benefits of asynchronous operation.

5. Experiments

5.1. Setups

Hardware. Our experiments were conducted on 8 NVIDIA GeForce RTX 4090 (24GB) GPUs connected via PCIe, powered by 128 vCPU Intel (R) Xeon (R) Gold 6430 CPU.

Models and Datasets. We evaluate our approach on two configurations of the DiT-MoE model[7]: DiT-MoE-XL, which is configured with 8 experts across 28 layers, and DiT-MoE-G, with 16 experts across 40 layers, both containing 2 extra shared experts. DiT-MoE is trained on ImageNet, which we use as the benchmark for evaluation.

Baselines. To evaluate the effectiveness of our approach, we compare it against three baselines: *DistriFusion* [21] (displaced sequence parallelism), a state-of-the-art method for distributed diffusion models employing patch parallelism; *Expert Parallelism* [17], the standard approach for parallelizing MoE models; and *displaced expert parallelism*, which offsets expert processing to overlap communication and computation.

Metrics. We assess the performance of our method using several well-established metrics, including Fréchet Inception Distance (FID) [11], Sliced Fréchet Inception Distance (sFID) [27], Inception Score (IS) [32], as well as Precision and Recall [16]. FID and sFID measures distributional alignment, while IS, precision, and recall assess various aspects of sample quality.

Implementation Details. Our implementation is based on PyTorch 2.0.0+cu118 [28]. We utilize Rectified Flow [12, 23] for the DiT-MoE-XL and G models, as they are specifically trained to support this approach. The core codebase builds upon the original DiT-MoE implementation [5]. For expert parallelism, we referenced Fast-

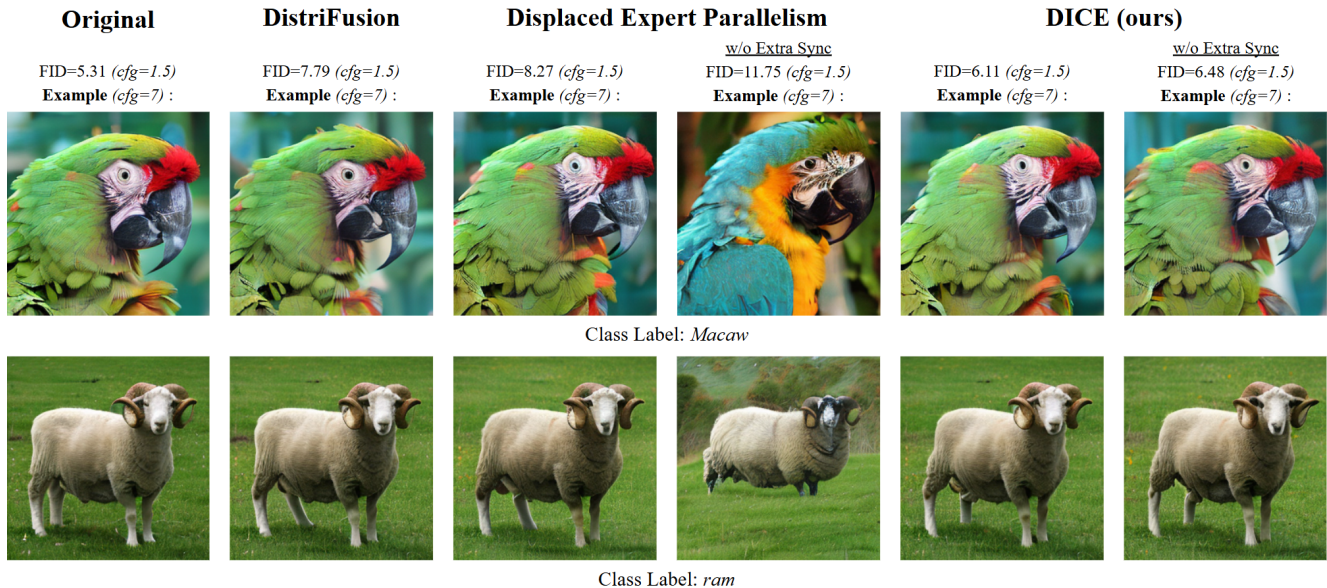


Figure 9. Qualitative results. DICE can reduce latency, increase throughput, save memory, and ensure that image quality is not affected. The default configuration uses a warmup of 6 steps, with periodical synchronization every 10 steps. W/o extra sync indicate no warmup and periodical synchronization applied.

Class-Conditional ImageNet 256×256					
Method	FID ↓	sFID ↓	IS ↑	Precision ↑	Recall ↑
Original	5.31	10.10	235.89	0.75	0.60
DistriFusion	7.79	12.13	206.24	0.72	0.59
Displaced Expert Parallelism	8.27	11.58	204.07	0.71	0.59
Interweaved Parallelism	6.97	11.01	216.62	0.72	0.59
DICE	6.11	10.93	225.65	0.73	0.59

Table 1. Quantitative evaluation. We employed Rectified Flow with 50 steps to generate 50K samples, evaluating on the ImageNet 256×256 dataset. All asynchronous methods apply 10 synchronized steps post cold start. The default configuration uses a warmup of 6 steps, with periodical synchronization every 10 steps but 10-steps warmup for DistriFusion.

MoE [9]. Sequence Parallelism [22] and DistriFusion [21] are adapted to DiT-MoE.

5.2. Main Results

Quality results. In Figure 9, we present qualitative results along with quantitative evaluations provided in Table 1. The images generated by DICE are nearly identical to the originals, indistinguishable from human perception.

Our method preserves the advantages of DistriFusion while achieving superior performance across all quality metrics, notably demonstrating a significantly lower FID of **6.11** compared to 7.79, while maintaining comparable performance to the Original in both precision and recall. Interweaved parallelism demonstrates a notable improvement in generation quality compared to displaced expert parallelism, primarily due to its effective mitigation of the stale-

ness issue.

Speedups and memory analysis. Our method effectively maintains the original quality while achieving a **1.2×** acceleration through expert parallelism. As demonstrated in Figure 10, DICE consistently exhibits significant speedups over expert parallelism across various batch sizes and image resolutions on both DiT-MoE-XL and G, reaching a maximum of **21%** when the batch size is 32. The observed acceleration primarily results from the overlap between communication and computation and the reduced data volume due to conditional communication. To further enhance image quality, we strategically trade off some inference efficiency relative to displaced expert parallelism. (**21.3%** vs. 25.8% speedup rates in XL model at batch size 32).

DICE consumes relatively less memory compared to other acceleration methods. Our method requires only half the buffer size of displaced parallelism. However, the mismatch between peak memory and buffer sizes makes the memory optimization less visible in the figure. Compared to DistriFusion, DICE demonstrates a more pronounced memory advantage. DistriFusion encounters out-of-memory issues in the XL model at batch sizes of 16 or more. Additionally, the large parameter size of the DiT-MoE-G model (around 33GB) prevents DistriFusion from running in our setup, highlighting the importance of expert parallelism for managing memory constraints effectively.

5.3. Ablation Study

Selective synchronization. Synchronizing deeper layers achieves the best image quality. We explore the impact

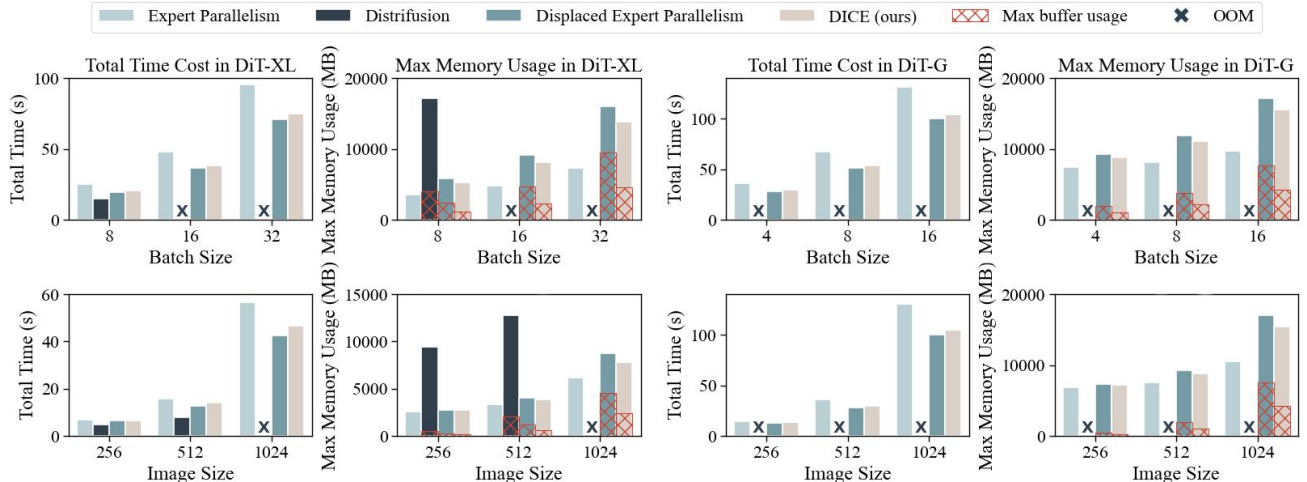


Figure 10. **Batch size scaling** and **Image size scaling** performance of DiT-MoE on 8 NVIDIA RTX 4090 GPUs, demonstrating the superior efficiency of DICE in terms of speed and memory usage.

Class-Conditional ImageNet 256×256					
Interweaved	Selective Sync	Conditional Comm	FID ↓	sFID ↓	IS ↑
✓	×	×	6.97	11.01	216.62
✓	Deep	×	5.74	10.53	230.23
✓	Shallow	×	6.55	10.63	221.61
✓	Staggered	×	5.95	10.39	227.78
✓	×	Low Score	7.24	11.26	214.10
✓	×	High Score	7.51	11.51	211.40
✓	×	Random	7.37	11.38	212.84

Table 2. Ablation quantitative evaluation. We applied various strategies to DICE to generate 50K samples, evaluated on the ImageNet 256×256 dataset. The rows sequentially compare different strategies for **selective synchronization** and **conditional communication**. The default configuration uses a warmup of 6 steps, with periodical synchronization every 10 steps.

of synchronizing different layers in mitigating layer-level staleness. As detailed in Table 2, we tested various synchronization strategies, including synchronizing the deeper half of the model layers (*Deep*), the shallower half (*Shallow*), and a staggered configuration where alternating layers are synchronized (*Staggered*). Results indicate that partial-async strategies outperform full-async method and *Deep* performs best, as it prioritizes synchronizing layers responsible for high-level semantics, which are more sensitive to staleness. This approach effectively balances latency with quality gains.

Conditional communication. Deprioritizing lower-score tokens (i.e., those less aligned with their assigned experts) reduces communication with minimal quality loss. To address token-level staleness, we experimented with selectively reducing communication frequency based on token importance, quantified by router scores. Specifically, we re-

duced the communication frequency for tokens with lower scores (*Low Score*), higher scores (*High Score*), and a random selection (*Random*), as shown in Table 2. Deprioritizing lower-score tokens consistently produced the best image quality. This finding validates that focusing on more critical tokens for frequent updates maximizes model performance, as these tokens contribute more significantly to the final output, achieving an effective trade-off between freshness and reduced communication.

Periodical synchronization. Periodical synchronization significantly improves image quality. As discussed in Section 4, periodical synchronization mitigates staleness propagation effectively. We compare interweaved parallelism with synchronization every 10 steps and no periodical synchronization, finding that Periodical Synchronization yields a superior FID of 6.97 compared to 7.43, with minimal increase in latency. Periodical synchronization reduces activation staleness, improving image quality, while periodical synchronization every 10 iterations further enhances quality with a marginal latency increase.

6. Conclusion

We propose DICE, a staleness-centric optimization framework that accelerates MoE-based diffusion model inference through three core innovations: *Interweaved Parallelism* for reducing step-level staleness, *Selective Synchronization* for selectively synchronizing staleness-sensitive layers, and *conditional caching*, a token-aware strategy that dynamically adjusts communication frequency. Together, these techniques reduce memory usage, enhance inference efficiency, and achieve up to 1.2× speedup over expert parallelism with minimal quality loss. We anticipate that DICE will pave the way for future scalability and efficiency improvements in distributed diffusion model inference.

References

- [1] Zigeng Chen, Xinyin Ma, Gongfan Fang, Zhenxiong Tan, and Xinchao Wang. AsyncDiff: Parallelizing Diffusion Models by Asynchronous Denoising, 2024. arXiv:2406.06911 [cs]. 3
- [2] Jia Deng, Wei Dong, Richard Socher, Li-Jia Li, Kai Li, and Li Fei-Fei. Imagenet: A large-scale hierarchical image database. In *2009 IEEE conference on computer vision and pattern recognition*, pages 248–255. Ieee, 2009. 3
- [3] Prafulla Dhariwal and Alexander Nichol. Diffusion models beat gans on image synthesis. *Advances in neural information processing systems*, 34:8780–8794, 2021. 1
- [4] Nan Du, Yanping Huang, Andrew M. Dai, Simon Tong, Dmitry Lepikhin, Yuanzhong Xu, Maxim Krikun, Yanqi Zhou, Adams Wei Yu, Orhan Firat, Barret Zoph, Liam Fedus, Maarten Bosma, Zongwei Zhou, Tao Wang, Yu Emma Wang, Kellie Webster, Marie Pellat, Kevin Robinson, Kathleen Meier-Hellstern, Toju Duke, Lucas Dixon, Kun Zhang, Quoc V. Le, Yonghui Wu, Zhifeng Chen, and Claire Cui. GLaM: Efficient Scaling of Language Models with Mixture-of-Experts, 2021. 1
- [5] Zhengcong Fei. feizc/DiT-MoE, 2024. original-date: 2024-06-25T08:27:55Z. 6
- [6] Zhengcong Fei, Mingyuan Fan, Changqian Yu, Debang Li, and Junshi Huang. Scaling diffusion transformers to 16 billion parameters. *arXiv preprint arXiv:2407.11633*, 2024. 1, 3
- [7] feizhengcong. feizhengcong/DiT-MoE · Hugging Face, 2024. 6
- [8] Amirhossein Habibiyan, Amir Ghodrati, Noor Fathima, Guillaume Sautiere, Rishiek Garrepalli, Fatih Porikli, and Jens Petersen. Clockwork diffusion: Efficient generation with model-step distillation. In *Proceedings of the IEEE/CVF Conference on Computer Vision and Pattern Recognition*, pages 8352–8361, 2024. 3
- [9] Jiaao He, Jiezhong Qiu, Aohan Zeng, Zhilin Yang, Jidong Zhai, and Jie Tang. FastMoE: A Fast Mixture-of-Expert Training System, 2021. arXiv:2103.13262 [cs]. 7
- [10] Jiaao He, Jidong Zhai, Tiago Antunes, Haojie Wang, Fuwen Luo, Shangfeng Shi, and Qin Li. Fastermoe: modeling and optimizing training of large-scale dynamic pre-trained models. In *Proceedings of the 27th ACM SIGPLAN Symposium on Principles and Practice of Parallel Programming*, page 120–134, New York, NY, USA, 2022. Association for Computing Machinery. 1, 4
- [11] Martin Heusel, Hubert Ramsauer, Thomas Unterthiner, Bernhard Nessler, and Sepp Hochreiter. Gans trained by a two time-scale update rule converge to a local nash equilibrium. In *Advances in Neural Information Processing Systems*. Curran Associates, Inc., 2017. 6
- [12] Jonathan Ho and Tim Salimans. Classifier-free diffusion guidance, 2022. 6
- [13] Jonathan Ho, Ajay Jain, and Pieter Abbeel. Denoising diffusion probabilistic models. *Advances in neural information processing systems*, 33:6840–6851, 2020. 1
- [14] Jonathan Ho, William Chan, Chitwan Saharia, Jay Whang, Ruiqi Gao, Alexey Gritsenko, Diederik P Kingma, Ben Poole, Mohammad Norouzi, David J Fleet, et al. Imagen video: High definition video generation with diffusion models. *arXiv preprint arXiv:2210.02303*, 2022. 1
- [15] Bahjat Kawar, Michael Elad, Stefano Ermon, and Jiaming Song. Denoising diffusion restoration models. *Advances in Neural Information Processing Systems*, 35:23593–23606, 2022. 1
- [16] Tuomas Kynkäänniemi, Tero Karras, Samuli Laine, Jaakko Lehtinen, and Timo Aila. Improved precision and recall metric for assessing generative models. In *Advances in Neural Information Processing Systems*. Curran Associates, Inc., 2019. 6
- [17] Dmitry Lepikhin, HyoukJoong Lee, Yuanzhong Xu, Dehao Chen, Orhan Firat, Yanping Huang, Maxim Krikun, Noam Shazeer, and Zhifeng Chen. GShard: Scaling Giant Models with Conditional Computation and Automatic Sharding, 2020. arXiv:2006.16668 [cs, stat]. 1, 4, 6
- [18] Mike Lewis, Shruti Bhosale, Tim Dettmers, Naman Goyal, and Luke Zettlemoyer. Base layers: Simplifying training of large, sparse models. In *Proceedings of the 38th International Conference on Machine Learning*, pages 6265–6274. PMLR, 2021. 1, 4
- [19] Jiamin Li, Yimin Jiang, Yibo Zhu, Cong Wang, and Hong Xu. Accelerating distributed MoE training and inference with lina. In *2023 USENIX Annual Technical Conference (USENIX ATC 23)*, pages 945–959, Boston, MA, 2023. USENIX Association. 1
- [20] Jing Li, Zhijie Sun, Xuan He, Li Zeng, Yi Lin, Entong Li, Binfan Zheng, Rongqian Zhao, and Xin Chen. Locmoe: A low-overhead moe for large language model training, 2024. 4
- [21] Muyang Li, Tianle Cai, Jiaxin Cao, Qinsheng Zhang, Han Cai, Junjie Bai, Yangqing Jia, Kai Li, and Song Han. DistriFusion: Distributed Parallel Inference for High-Resolution Diffusion Models. In *2024 IEEE/CVF Conference on Computer Vision and Pattern Recognition (CVPR)*, pages 7183–7193, Seattle, WA, USA, 2024. IEEE. 2, 3, 5, 6, 7
- [22] Shenggui Li, Fuzhao Xue, Chaitanya Baranwal, Yongbin Li, and Yang You. Sequence Parallelism: Long Sequence Training from System Perspective, 2022. arXiv:2105.13120 [cs]. 7
- [23] Xingchao Liu, Chengyue Gong, and Qiang Liu. Flow straight and fast: Learning to generate and transfer data with rectified flow, 2022. 6
- [24] Zhengxiong Luo, Dayou Chen, Yingya Zhang, Yan Huang, Liang Wang, Yujun Shen, Deli Zhao, Jingren Zhou, and Tieniu Tan. Videofusion: Decomposed diffusion models for high-quality video generation. *arXiv preprint arXiv:2303.08320*, 2023. 1
- [25] Xinyin Ma, Gongfan Fang, Michael Bi Mi, and Xinchao Wang. Learning-to-Cache: Accelerating Diffusion Transformer via Layer Caching, 2024. arXiv:2406.01733 [cs]. 3, 4
- [26] Xinyin Ma, Gongfan Fang, and Xinchao Wang. Deepcache: Accelerating diffusion models for free. In *Proceedings of the IEEE/CVF Conference on Computer Vision and Pattern Recognition (CVPR)*, pages 15762–15772, 2024. 3, 4

- [27] Charlie Nash, Jacob Menick, Sander Dieleman, and Peter W. Battaglia. Generating images with sparse representations. *ArXiv*, abs/2103.03841, 2021. 6
- [28] Adam Paszke, Sam Gross, Francisco Massa, Adam Lerer, James Bradbury, Gregory Chanan, Trevor Killeen, Zeming Lin, Natalia Gimelshein, Luca Antiga, Alban Desmaison, Andreas Kopf, Edward Yang, Zachary DeVito, Martin Raison, Alykhan Tejani, Sasank Chilamkurthy, Benoit Steiner, Lu Fang, Junjie Bai, and Soumith Chintala. Pytorch: An imperative style, high-performance deep learning library. In *Advances in Neural Information Processing Systems 32*, pages 8024–8035. Curran Associates, Inc., 2019. 6
- [29] William Peebles and Saining Xie. Scalable diffusion models with transformers. In *Proceedings of the IEEE/CVF International Conference on Computer Vision (ICCV)*, pages 4195–4205, 2023. 1
- [30] Samyam Rajbhandari, Conglong Li, Zhewei Yao, Minjia Zhang, Reza Yazdani Aminabadi, Ammar Ahmad Awan, Jeff Rasley, and Yuxiong He. DeepSpeed-MoE: Advancing mixture-of-experts inference and training to power next-generation AI scale. In *Proceedings of the 39th International Conference on Machine Learning*, pages 18332–18346. PMLR, 2022. 1, 3, 4, 5
- [31] Robin Rombach, Andreas Blattmann, Dominik Lorenz, Patrick Esser, and Björn Ommer. High-resolution image synthesis with latent diffusion models. In *Proceedings of the IEEE/CVF conference on computer vision and pattern recognition*, pages 10684–10695, 2022. 1
- [32] Tim Salimans, Ian Goodfellow, Wojciech Zaremba, Vicki Cheung, Alec Radford, Xi Chen, and Xi Chen. Improved techniques for training gans. In *Advances in Neural Information Processing Systems*. Curran Associates, Inc., 2016. 6
- [33] Pratheba Selvaraju, Tianyu Ding, Tianyi Chen, Ilya Zharkov, and Luming Liang. FORA: Fast-Forward Caching in Diffusion Transformer Acceleration, 2024. arXiv:2407.01425 [cs]. 3
- [34] Noam Shazeer, Azalia Mirhoseini, Krzysztof Maziarz, Andy Davis, Quoc Le, Geoffrey Hinton, and Jeff Dean. Outrageously Large Neural Networks: The Sparsely-Gated Mixture-of-Experts Layer, 2017. arXiv:1701.06538 [cs, stat]. 1, 3
- [35] Uriel Singer, Adam Polyak, Thomas Hayes, Xi Yin, Jie An, Songyang Zhang, Qiyuan Hu, Harry Yang, Oron Ashual, Oran Gafni, et al. Make-a-video: Text-to-video generation without text-video data. *arXiv preprint arXiv:2209.14792*, 2022. 1
- [36] Junhyuk So, Jungwon Lee, and Eunhyeok Park. Frdiff: Feature reuse for universal training-free acceleration of diffusion models. *arXiv preprint arXiv:2312.03517*, 2023. 3
- [37] Jiaming Song, Chenlin Meng, and Stefano Ermon. Denoising diffusion implicit models. *arXiv preprint arXiv:2010.02502*, 2020. 1
- [38] Arash Vahdat, Karsten Kreis, and Jan Kautz. Score-based generative modeling in latent space. *Advances in neural information processing systems*, 34:11287–11302, 2021. 1
- [39] Ashish Vaswani, Noam Shazeer, Niki Parmar, Jakob Uszkoreit, Llion Jones, Aidan N Gomez, Łukasz Kaiser, and Illia Polosukhin. Attention is all you need. In *Advances in Neural Information Processing Systems*. Curran Associates, Inc., 2017. 1
- [40] Jiannan Wang, Jiarui Fang, Aoyu Li, and PengCheng Yang. PipeFusion: Displaced Patch Pipeline Parallelism for Inference of Diffusion Transformer Models, 2024. arXiv:2405.14430 [cs]. 3, 5
- [41] Felix Wimbauer, Bichen Wu, Edgar Schoenfeld, Xiaoliang Dai, Ji Hou, Zijian He, Artsiom Sanakoyeu, Peizhao Zhang, Sam Tsai, Jonas Kohler, et al. Cache me if you can: Accelerating diffusion models through block caching. In *Proceedings of the IEEE/CVF Conference on Computer Vision and Pattern Recognition*, pages 6211–6220, 2024. 3
- [42] Jinghan Yao, Quentin Anthony, Aamir Shafi, Hari Subramoni, and Dhableswar K. DK Panda. Exploiting Inter-Layer Expert Affinity for Accelerating Mixture-of-Experts Model Inference. In *2024 IEEE International Parallel and Distributed Processing Symposium (IPDPS)*, pages 915–925, Los Alamitos, CA, USA, 2024. IEEE Computer Society. 1, 4

DICE: Staleness-Centric Optimizations for Efficient Diffusion MoE Inference

Supplementary Material

7. More Implementation Details

System Setup. The models used in our study are the latest publicly available versions of DiT-MoE from Huggingface. In our experimental results, the batch size refers to the local batch size, representing the number of samples processed per device.

Expert Score Scaling. There are two approaches for scaling results after expert processing: (1) using the latest router scores computed in the current step, which provides fresher scores, and (2) using the router scores corresponding to the stale expert input, offering better alignment with the activations used. The selection of the scores has little impact on performance. For fairness, both displaced parallelism and DICE use the stale router scores for scaling.

Extending Image Sizes. The public DiT-MoE model supports only 256×256 image sizes. To extend our experiments to larger images, we initialize positional embeddings for other sizes. Although this adjustment prevents the model from generating meaningful images, it enables us to evaluate latency, memory usage and speedup across different resolutions.

8. Discussion

Limitations. Although DICE demonstrates significant gains in inference efficiency, there remain avenues for further improvements. Optimized kernels and more efficient NCCL operations could help further reduce latency. Additionally, integrating DICE with existing expert parallelism optimizations offers opportunities to enhance its efficiency and scalability. Another limitation lies in the availability of MoE-based diffusion models, which restricts our evaluations to a limited set of configurations. As more MoE-based diffusion models are developed, DICE can be validated and refined across a broader range of scenarios.

Influence of Shared Experts. The architecture of DiT-MoE includes shared experts, a proven mechanism for enhancing MoE performance. We hypothesize that these shared experts may help mitigate the impact of staleness in similarity-based asynchronous parallelism. Unlike routed experts, whose outputs can become stale, the shared expert’s computations are always up-to-date, potentially providing fresh information to balance the delayed outputs from routed experts. This characteristic might play a role in the performance of DICE, particularly when compared to DistriFusion. While both approaches exhibit a staleness of 1, DICE confines staleness to routed experts while benefiting from the shared expert’s fresh contributions. This suggests a possible advantage for DICE in MoE-based models.

9. More Experiment Results

Setups. The extra experiments were conducted on 8 NVIDIA RTX 3080 (20GB) GPUs¹ connected via PCIe, powered by 96 vCPU Intel(R) Xeon(R) Platinum 8352V CPU @ 2.10GHz, with 384GB of memory.

Quality results. In Figure 12, we present additional qualitative results across six different classes. Notably, only the displaced expert parallelism without extra synchronization demonstrates considerable deviations. In particular, the images produced by DICE closely resemble the original ones.

Speedups and memory analysis. The results shown in Figure 13 and 14. Similar to the results on the NVIDIA RTX 4090 GPUs, DICE also demonstrates significant speedup across various batch sizes and image resolutions, achieving a maximum speedup of 18% at batch size 32. The speedup on the 3080 GPUs is slightly lower than on the 4090 GPUs under the same configuration (21%). This may be due to the 3080’s lower computational performance, which reduces the impact of communication overhead on overall inference time.

10. Latency-Quality Trade-Off.

Figure 11 illustrates the comparison between our proposed methods and baseline approaches. Our method, DICE, balances latency and image quality, significantly improving FID scores while maintaining competitive inference time.

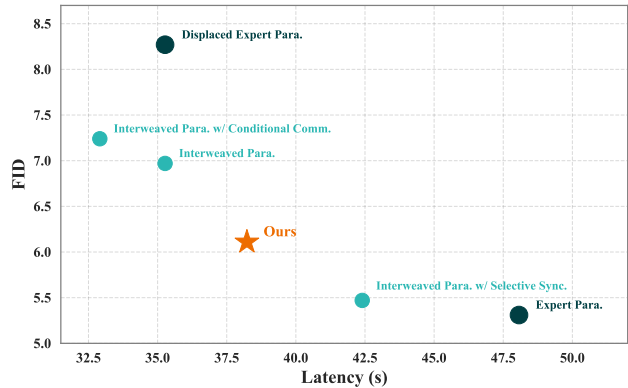


Figure 11. Trade-off among proposed optimizations. We demonstrate the individual benefits of each technique. Baselines are shown in dark colors, with latency measured on NVIDIA RTX 4090 GPUs with batch size 16.

¹Conducted on GPUs rented from the AutoDL(<https://www.autodl.com/home>), which may potentially include non-standard or modified configurations.



Figure 12. Extra qualitative results. The default configuration uses a warmup of 6 steps, with periodical synchronization every 10 steps. W/o extra sync indicates no warmup and periodical synchronization applied.

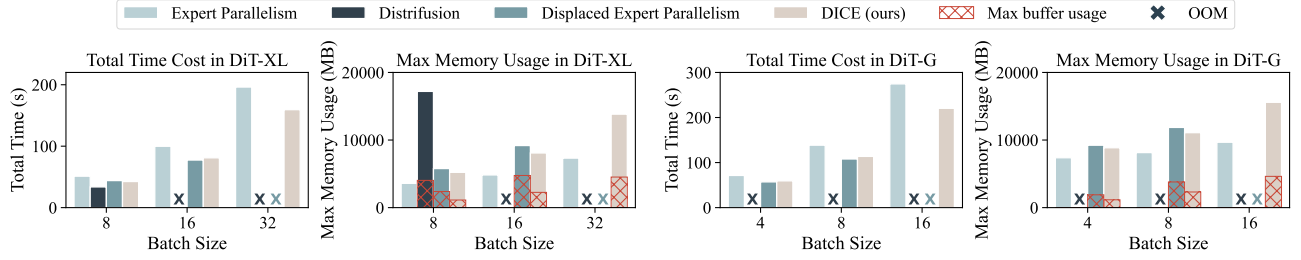


Figure 13. **Batch size scaling** performance of DiT-MoE on 8 NVIDIA RTX 3080 GPUs.

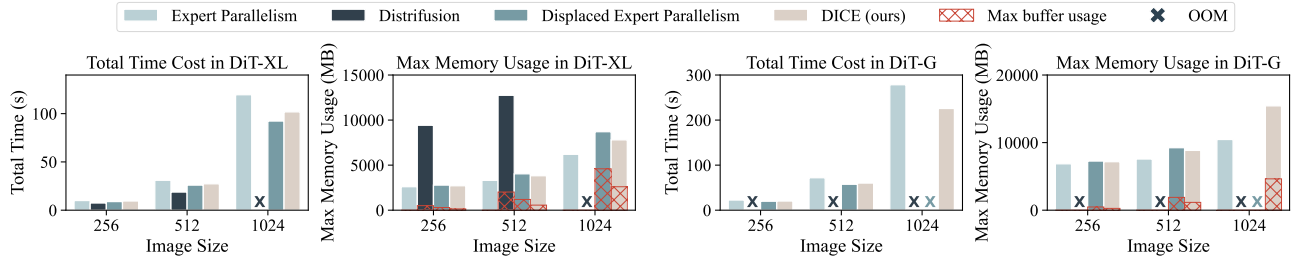


Figure 14. **Image size scaling** performance of DiT-MoE on 8 NVIDIA RTX 3080 GPUs.